

## ac conductivity of $\text{Sb}_2\text{O}_3\text{-P}_2\text{O}_5$ glasses

A. Datta, Anit K. Giri, and D. Chakravorty

*Indian Association for the Cultivation of Science, Jadavpur, Calcutta 700 032, India*

(Received 6 January 1992; revised manuscript received 1 October 1992)

ac resistivity has been measured for glasses in the system  $(\text{Sb}_2\text{O}_3)_x(\text{P}_2\text{O}_5)_{(1-x)}$  with  $0.03 < x < 0.2$  over a frequency range 2–100 kHz for temperatures varying from 100 to 350 K. The resistivity shows a frequency dependence given by  $\rho(\omega) \propto \omega^{-s}$  with  $s$  having values in the range 0.8–0.95. The conductivity in these glasses arises due to the presence of  $\text{Sb}^{3+}$  and  $\text{Sb}^{5+}$  ions. A correlated-barrier-hopping model of bipolarons predicts hopping-length values which are inconsistent with the overall concentration of antimony ions in the glasses concerned. The overlapping-large-polaron model, on the other hand, gives the correct variation of tunneling distance with glass composition.

### I. INTRODUCTION

Semiconducting properties in oxide glasses containing transition-metal ions originate as a result of the presence of two valence states of these ions in the glass matrix, e.g.,  $\text{V}^{4+}/\text{V}^{5+}$ ,  $\text{Fe}^{2+}/\text{Fe}^{3+}$ , and  $\text{Cu}^+/\text{Cu}^{2+}$ .<sup>1–3</sup> Electronic conduction in these glasses has been shown to arise from a small-polaron-hopping mechanism. In silicate and borate glasses containing antimony and arsenic oxide, respectively, the latter have been shown to exist in two valence states, viz.,  $\text{Sb}^{3+}/\text{Sb}^{5+}$  and  $\text{As}^{3+}/\text{As}^{5+}$ . Such ion pairs contribute to electrical conduction in these glasses by the mechanism of hopping of a pair of electrons (bipolarons) between the two ion sites concerned.<sup>4–7</sup> A correlated-barrier-hopping (CBH) model has been invoked to explain the nature of ac-resistivity variation in these glasses. We have carried out transport-property measurements on glasses in the system  $(\text{Sb}_2\text{O}_3)_x(\text{P}_2\text{O}_5)_{(1-x)}$  with  $0.03 < x < 0.2$ . The ac-resistivity data in the temperature range 100–350 K indicate that an overlapping-large-polaron-tunneling (OLPT) mechanism is operative in this glass system. Such a mechanism, although predicted theoretically, has been found to be present in only a very few systems.<sup>8</sup> We report the details of our investigation in the present paper.

### II. EXPERIMENT

The glasses were prepared by melting AR-grade chemicals. Antimony was introduced as  $\text{Sb}_2\text{O}_3$  and  $\text{P}_2\text{O}_5$  was derived from  $(\text{NH}_4)_2\text{HPO}_4$ . Calculated amounts of these chemicals were taken in an alumina crucible and the mixture was melted in an electrically heated furnace at a temperature around 1470 K. Glasses were cast by pouring the melt onto an aluminium plate. The amounts of antimony ions present in the two valence states were determined by chemical analysis. The glass sample (~2 g) was first dissolved in a mixture of distilled water and NaOH. The solution was stirred continuously for 30 min. Dilute  $\text{H}_2\text{SO}_4$  was then added to the solution drop by drop until the latter showed a pH value equal to 1. The solution was titrated with 0.02N  $\text{KMnO}_4$  and the

amount of  $\text{Sb}^{3+}$  ions present was determined.<sup>9,10</sup>

To determine the amount of  $\text{Sb}^{5+}$  ions the glass solution prepared as above was mixed with about 5 g of potassium iodide. A small amount of sodium bicarbonate was dissolved in the mixture for creating an atmosphere of  $\text{CO}_2$ . This solution was then titrated with 0.01N sodium thiosulphate using starch solution as an indicator. Table I gives the glass compositions and the values of  $[\text{Sb}^{5+}]/[\text{Sb}^{3+}]$  as obtained by chemical analysis for the different glasses. The figures within parentheses in this table indicate the starting composition of the glass concerned. It is evident that there is a substantial loss of antimony oxide by volatilization during the melting process.

The densities of the different glasses were determined by Archimedes principle using acetone as the liquid. The total concentration  $N_t$  of antimony ions was estimated from the density value and the glass composition concerned. The average separation  $R$  between the antimony ions within the glass was calculated from the equation

$$R = \left[ \frac{3}{4\pi N_t} \right]^{1/3}. \quad (1)$$

In Table II the density, antimony ion concentration, and average intersite separation are shown.

For electrical measurements glass samples of dimension 1 cm × 1 cm × 2 mm were used. After polishing the surfaces they were painted with silver electrodes (supplied by Acheson Colloiden B. V. Netherlands). ac measurements were carried out in a General Radio 1615-A capacitance bridge over a frequency range 2–100 kHz for temperatures varying from 100 to 350 K. The sample holder used has been described earlier.<sup>4</sup>

TABLE I. Compositions of the glasses investigated.

Glass no.	$\text{P}_2\text{O}_5$ (mol %)	$\text{Sb}_2\text{O}_3$ (mol %)	$[\text{Sb}^{5+}]/[\text{Sb}^{3+}]$
1	96.9(90)	3.1(10)	0.003
2	88.3(80)	11.7(20)	0.009
3	80.1(70)	19.9(30)	0.045

TABLE II. Density, intersite separation, and antimony ion concentration in different glasses.

Glass no.	Density $\text{g cm}^{-3}$	Antimony concentration $N_t$ ( $\text{cm}^{-3}$ )	Average intersite separation $R$ ( $\text{\AA}$ )
1	2.95	$7.5 \times 10^{20}$	6.8
2	3.42	$3.0 \times 10^{21}$	4.3
3	3.89	$5.4 \times 10^{21}$	3.5

### III. RESULTS

Figures 1–3 show the variation of ac resistivity as a function of inverse temperature for glass nos. 1, 2, and 3, respectively. The symbols represent the experimental data. The continuous lines merely indicate the trend of resistivity variation. All samples exhibit a lowering of resistivity as the temperature is increased. Also, there is a gradual decrease in activation energy as the temperature is reduced. It is to be noted that there is a sharp decrease in resistivity at around 280 K observed for glass no. 3. This is ascribed to the presence of a higher fraction of antimony ions in the pentavalent state in this glass as compared to the other two glass compositions. This will be apparent when we discuss the model for transport in the present glass system in the following section.

The ac resistivity of all the glasses has been found to obey the relation

$$\rho(\omega) \propto \omega^{-s}, \quad (2)$$

where  $\omega$  is the angular frequency and  $s$  is the exponent. By a least-squares fitting of these data we find the value of

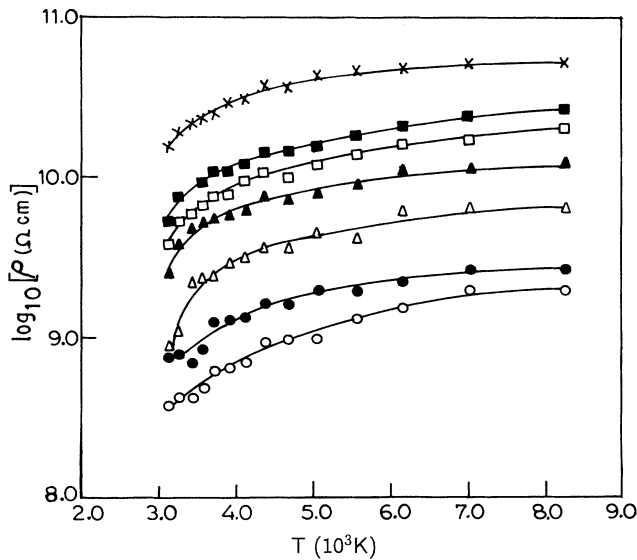


FIG. 1. Variation of ac resistivity as a function of temperature for glass no. 1. The curves are for the following data: 2, 5, 7, 10, 20, 50, and 100 kHz.

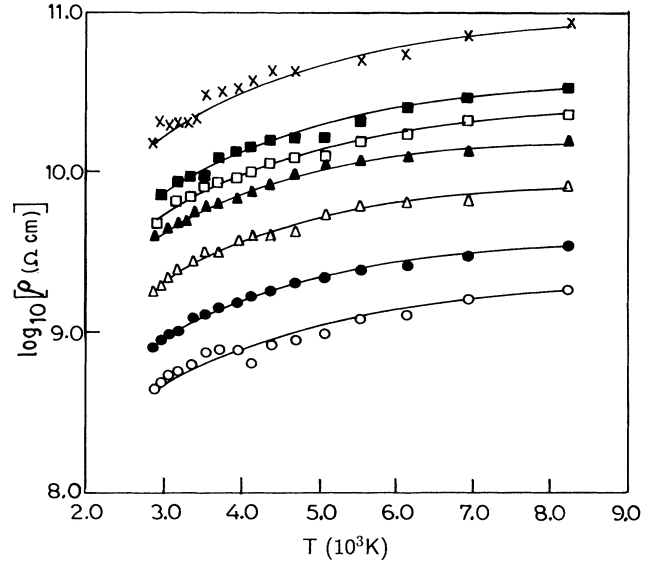


FIG. 2. Variation of ac resistivity as a function of temperature for glass no. 2. The curves are for the following data: 2, 5, 7, 10, 20, 50, and 100 kHz.

$s$  to be nearly unity (in the range 0.8–0.95) for all the glasses. In order to determine the physical model which explains our data we have carried out detailed analysis as described in the following section.

### IV. DISCUSSION

We have used two different models which were discussed by us earlier to explain the ac-conductivity behavior of silicate glasses containing  $\text{Sb}^{5+}$  and  $\text{Sb}^{3+}$  ions.<sup>11</sup>

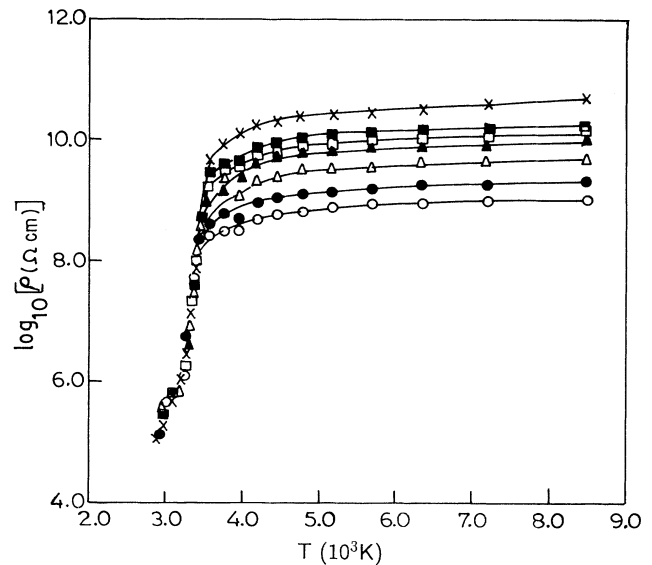


FIG. 3. Variation of ac resistivity as a function of temperature for glass no. 3. The curves are for the following data: 2, 5, 7, 10, 20, 50, and 100 kHz.

In the correlated-barrier-hopping model<sup>8</sup> in the present system two electrons hop simultaneously between the defect sites represented by  $\text{Sb}^{3+}$  and  $\text{Sb}^{5+}$  ions, respectively. The ac resistivity has the following expression:

$$\rho(\omega) = 12 / [\pi^3 N^2 \epsilon \epsilon_0 \omega R_\omega^6], \quad (3)$$

where  $N$  is the spatial density of localized states,  $\epsilon$  the dielectric constant of the glass,  $\epsilon_0$  the free-space permittivity,  $\omega$  the angular frequency, and  $R_\omega$  the hopping length. The value of  $R_\omega$  is given by the equation

$$R_\omega = 2e^2 / [\pi \epsilon \epsilon_0 (W_M + kT \ln \omega \tau_0)], \quad (4)$$

where  $e$  is the electronic charge,  $W_M$  the barrier height at infinite intersite separation,  $k$  the Boltzmann constant,  $T$  the temperature, and  $\tau_0$  a characteristic relaxation time which is assumed to have a value of the order of inverse phonon frequency. The frequency exponent  $s$  is given by

$$s = 1 - [6kT / (W_M + kT \ln \omega \tau_0)]. \quad (5)$$

The experimental ac-resistivity results were fitted to the above equations using  $W_M$ ,  $\tau_0$ , and  $N$  as parameters. In Fig. 4 we show the theoretical curves fitted to the experimental data at five different temperatures for glass no. 2. These are typical for all the glasses at different temperatures. The symbols represent the data points and the solid lines the least-squares-fitted curves. The parameters obtained in the case of different glasses are summarized in Table III. The values of  $R$  have been calculated from Eq. (4) using the values of these parameters. It is evident from these values that the hopping length  $R_\omega$  is predicted in this model to increase as the antimony concentration increases in the glass. The density  $N$  of localized states, on the other hand, shows a decreasing trend with antimony concentration. Such results are obviously inconsistent with the physical situation. It is concluded therefore that the CBH model does not hold well in the present glass system.

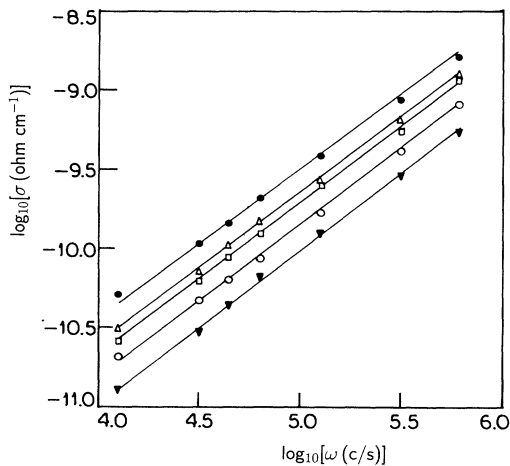


FIG. 4. Variation of conductivity as a function of frequency at different temperatures for glass no. 2. The curves are for the following data: 300, 252, 227, 180, and 121 K. Theoretical curve by CBH model.

TABLE III. Parameters obtained from the CBH model by least-squares fitting.

Glass no.	$\tau_0$ (sec)	$W_M$ (eV)	$R_\omega$ (Å)	$N$ ( $\text{cm}^{-3}$ )
1	$1.3 \times 10^{-13}$	2.78	5.0	$2.4 \times 10^{20}$
2	$1.4 \times 10^{-13}$	2.56	7.0	$8.5 \times 10^{19}$
3	$1.0 \times 10^{-13}$	1.34	11.9	$1.9 \times 10^{19}$

We now consider the overlapping-large-polaron-tunneling mechanism.<sup>12</sup> In this case the spatial extent of the polarons is supposed to be large compared to interatomic spacing. The polaron-hopping energy  $W_H$  in this model is given by the following equation:

$$W_H = W_{HO} (1 - r_0/R), \quad (6)$$

where  $r_0$  is the radius of the large polaron,  $W_{HO}$  is a constant, and  $R$  is the intersite distance.

The ac resistivity in this case is given by

$$\rho(\omega) = \frac{12[2\alpha kT + W_{HO} r_0 / R_\omega^2]}{\pi^4 e^2 (kT)^2 [N(E_F)]^2 \omega R_\omega^4}, \quad (7)$$

where  $\alpha^{-1}$  is the spatial decay constant for the localized electron wave function,  $N(E_F)$  the density of localized states at the Fermi level, and  $R_\omega$  the tunneling distance at angular frequency  $\omega$  and is given by the expression

$$R_\omega = \frac{1}{4\alpha} \left\{ \ln(1/\omega\tau_0) - W_{HO}/kT + \left[ \left[ \ln \left( \frac{1}{\omega\tau_0} \right) - \frac{W_{HO}}{kT} \right]^2 + \frac{8\alpha r_0 W_{HO}}{kT} \right]^{1/2} \right\}. \quad (8)$$

The frequency exponent  $s$  is obtained from the following equation:

$$s = 1 - \frac{8R_\omega\alpha + 6r_0 W_{HO}/R_\omega kT}{(2R_\omega\alpha + r_0 W_{HO}/R_\omega kT)^2}. \quad (9)$$

The experimental data were fitted to the above equations using  $\tau_0$ ,  $W_{HO}$ ,  $r_0$ ,  $\alpha$ , and  $N(E_F)$  as the parameters. Figure 5 shows the theoretical curves fitted to the experimental data at five temperatures for glass no. 2. These are typical for all the glasses at different temperatures. The symbols represent the data points and the continuous lines the least-squares-fitted curves. The parameters as determined in the case of different glasses are summarized in Table IV. The values of  $R_\omega$  have been calculated

TABLE IV. Parameters obtained from the OLPT model by least-squares fitting.

Glass no.	$\tau_0$ (sec)	$W_{HO}$ (eV)	$r_0$ (Å)	$\alpha^{-1}$ (Å)	$R_\omega$ (Å)	$N(E_F)$ ( $\text{eV}^{-1} \text{cm}^{-3}$ )
1	$1.3 \times 10^{-13}$	1.4	14.5	0.6	14.9	$3.5 \times 10^{20}$
2	$1.3 \times 10^{-13}$	0.9	7.5	0.6	8.8	$8.9 \times 10^{20}$
3	$1.3 \times 10^{-13}$	0.5	6.7	0.7	8.3	$1.1 \times 10^{21}$

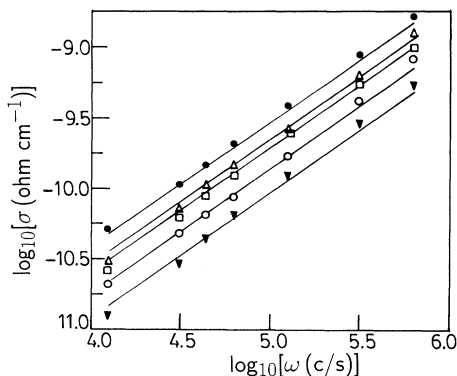


FIG. 5. Variation of conductivity as a function of frequency at different temperatures for glass no. 2. The curves are for the following data: 300, 252, 227, 180, and 121 K. Theoretical curve by OLPT model.

from Eq. (8) using the values of these parameters. Figure 6 shows the variation of  $s$  as a function of temperature for glass no. 2. The fit between theory and experiment is satisfactory. This is typical of the other glasses also. The value of  $W_{HO}$  decreases as the  $\text{Sb}_2\text{O}_3$  concentration is increased in the glass system. This is due to the increase in glass density which brings about an increase in the dielectric permittivity of the glasses containing a higher mole fraction of antimony ions. Such an increase will cause the polaron-hopping energy for  $R \rightarrow \infty$  to decrease because of the electrostatic nature of interaction involved.<sup>12</sup> These results give  $R_\omega$  values which are consistent with the antimony concentration in the different glasses. It is therefore concluded that the OLPT mechanism controls the low-temperature ac-resistivity behavior in the present glass system. The number of antimony sites participating in the OLPT mode of conduction is estimated from  $KTN(E_F)$  with  $T \sim 300$  K. The values are found to be  $9.1 \times 10^{18} \text{ cm}^{-3}$ ,  $2.3 \times 10^{19} \text{ cm}^{-3}$ , and  $2.7 \times 10^{19} \text{ cm}^{-3}$  for glasses 1, 2, and 3, respectively. It is evident therefore that only a small fraction of the total antimony ions present in the glasses contribute to the conduction mechanism. This is believed to arise due to some of the antimony ion sites being rendered inactive by some complex formation.<sup>13</sup> In the present case, we can visualize the formation of a structure like the following:

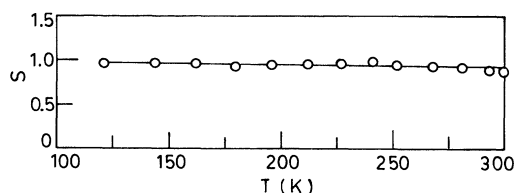
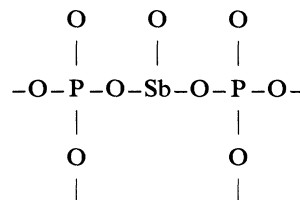


FIG. 6. Variation of  $s$  as a function of temperature for glass no. 2. (○) Experimental data; OLPT model.



The above structure is constructed keeping in view the fourfold coordination exhibited by phosphate glasses.<sup>14</sup> The  $\text{Sb}^{3+}$  and  $\text{Sb}^{5+}$  ions occupying the interstitial sites contribute to the electron hopping transport. From the low values of  $[\text{Sb}^{5+}]/[\text{Sb}^{3+}]$  as estimated for the present series of glasses it appears that most of the  $\text{Sb}^{3+}$  ions take part in the above complex formation. As a consequence, the effective intersite separation between the antimony ions contributing to bipolaronic conduction should be higher than that estimated from the chemical composition of these glasses. This is, in fact, borne out by the large values of  $R_\omega$  shown in Table IV as compared to the  $R$  values given in Table II.

An interesting feature of the present results is that in a related glass system, viz.,  $\text{Sb}_2\text{O}_3\text{-SiO}_2$ , the CBH model was found to hold in the temperature range 170–290 K.<sup>11</sup> Evidently the difference between the two systems lies in the network formers used in these glasses. We have calculated the value of mean electronegativity difference  $\bar{x}$  between oxygen and the other atoms in these glasses from the following relation:

$$\bar{x} = \frac{(X_O - X_{\text{Sb}}) + (X_O - X_{\text{P/Si}})}{2}, \quad (10)$$

where  $X_O$ ,  $X_{\text{Sb}}$ , and  $X_{\text{P/Si}}$  represent the Pauling electronegativities of oxygen, antimony, and phosphorous (or silicon as the case may be) atoms, respectively.<sup>15</sup> In the case of  $\text{Sb}_2\text{O}_3\text{-P}_2\text{O}_5$  system  $\bar{x} = 1.5$ , whereas for  $\text{Sb}_2\text{O}_3\text{-SiO}_2$  system  $\bar{x} = 1.7$ . A lower value of  $\bar{x}$  means the bond between oxygen and other atoms will tend to become more covalent. This will mean a larger spatial distribution of the outer electrons with respect to the interatomic separation. As a result the effective value of  $\alpha^{-1}$  will be higher in the case of the  $\text{Sb}_2\text{O}_3\text{-P}_2\text{O}_5$  system than that in the  $\text{Sb}_2\text{O}_3\text{-SiO}_2$  glasses. Such a situation should make the OLPT mechanism operative in the case of  $\text{Sb}_2\text{O}_3\text{-P}_2\text{O}_5$  glasses whereas the CBH mechanism should be predominant in  $\text{Sb}_2\text{O}_3\text{-SiO}_2$  glass systems.

In summary, the ac-resistivity characteristics of glasses in the system  $(\text{Sb}_2\text{O}_3)(\text{P}_2\text{O}_5)_{(1-x)}$  with  $0.03 < x < 0.2$  have been reported. The resistivity obeys a  $\omega^{-s}$  variation. The resistivity variation as a function of frequency and of temperature has been analyzed on the basis of both CBH and OLPT models. The least-squares-fitted parameters deduced from the OLPT model are consistent with the intersite separation as expected from the chemical compositions of the different glasses.

#### ACKNOWLEDGMENTS

A.D. thanks the Council of Scientific and Industrial Research, Government of India for support. The work has been supported by a grant from the National Science Foundation, Washington, D.C. through the special Foreign Currency Program.

- <sup>1</sup>C. F. Drake and L. F. Scanlan, *J. Non-Cryst. Solids* **4**, 234 (1970).
- <sup>2</sup>L. Murawski, C. H. Chung, and J. D. Mckenzie, *J. Non-Cryst. Solids* **32**, 91 (1979).
- <sup>3</sup>A. Ghosh and D. Chakravorty, *J. Phys. Condens. Matter* **2**, 5365 (1990).
- <sup>4</sup>D. Chakravorty, D. Kumar, and G. V. S. Sastry, *J. Phys. D* **12**, 2209 (1979).
- <sup>5</sup>D. Kumar and D. Chakravorty, *J. Phys. D* **13**, 1331 (1980).
- <sup>6</sup>D. Chakravorty and L. G. Kishore Kumar, *J. Phys. D* **15**, 1089 (1982).
- <sup>7</sup>B. Dutta and D. E. Day, *J. Non-Cryst. Solids* **48**, 345 (1982).
- <sup>8</sup>S. R. Elliott, *Adv. Phys.* **36**, 135 (1987).
- <sup>9</sup>P. Close, H. M. Shephard, and C. M. Drummond, *J. Am. Ceram. Soc.* **41**, 455 (1958).
- <sup>10</sup>A. I. Vogel, *Textbook Quantitative Inorganic Analysis* (Longman, New York, 1978), p. 383.
- <sup>11</sup>A. Datta, Anit K. Giri, and D. Chakravorty, *J. Phys. Condens. Matter* **4**, 1783 (1992).
- <sup>12</sup>A. R. Long, *Adv. Phys.* **31**, 553 (1982).
- <sup>13</sup>G. S. Linsley, A. E. Owen, and F. M. Hayatee, *J. Non-Cryst. Solids* **4**, 208 (1970).
- <sup>14</sup>W. D. Kingery, *Introduction to Ceramics* (Wiley, New York, 1967), p. 156.
- <sup>15</sup>L. Pauling, *The Nature of the Chemical Bond* (Cornell University Press, Ithaca, New York, 1945), p. 64.